Expanded Stability through Higher Temporal Accuracy for Time-Centered Advection Schemes

RICHARD J. BABARSKY

Department of Mathematics, James Madison University, Harrisonburg, Virginia

ROBERT SHARPLEY

Department of Mathematics, University of South Carolina, Columbia, South Carolina

(Manuscript received 14 August 1995, in final form 17 September 1996)

ABSTRACT

Applying standard explicit time-differencing to hyperbolic equations (i.e., which characterize convection-dominated atmospheric flows) invariably results in rather severe stability restrictions. The primary problem appears to be attributable to the differencing approximation of the time derivative term. In this study the authors show that, for explicit, time-centered advection schemes, achieving higher-order temporal accuracy results in schemes with significantly improved stability properties compared with conventional leapfrog methods. Linear results show that marked improvement is possible in the stability properties by including in the differencing scheme a crucial term approximating the time derivative of third order. The critical CFL number for this time-centered Taylor (TCT) scheme is shown to exceed that of second-order leapfrog by nearly a factor of 2. Similar results hold for the corresponding fourth-order schemes. A solid-body rotation test confirms the findings of the two-dimensional stability analysis and compares these time-centered schemes with popular forward-in-time methods. One-dimensional nonlinear results corroborate the fundamental stablizing effect of the TCT approach with the TCT algorithm offering significant improvements in nonlinear stability over leapfrog methods as well as MacCormack's scheme—a popular nonlinear, dissipative differencing scheme.

1. Introduction

This paper explores the application of explicit, time-centered schemes to modeling advection processes. Along with the forward-in-time Lax–Wendroff-type schemes, leapfrog schemes have been extensively used in meteorological models. In fact leapfrog has been considered by many as the scheme of choice for large-scale atmospheric models. Reasons typically cited for this choice are its simplicity (leapfrog is a straightforward one-step scheme), its zero implicit diffusion (which is common to all time-centered schemes), and its conservation properties. On the other hand, due to its lack of intrinsic dissipation, it exhibits rather poor dispersive properties that are exacerbated in the context of modeling nonlinear convection. Recent work by Mendez-Nunez and Carroll (1993) has focused on the shortcomings of the leapfrog scheme, especially when applied to nonlinear equations modeling localized, nonsmooth phenomena. In this study we derive several alternative time-centered schemes which will be evaluated, along with the classic leapfrog scheme, under a variety of different conditions. In particular, a family of time-centered Taylor (TCT) algorithms are derived which achieve higher temporal accuracy than standard leapfrog schemes and exhibit superior stability characteristics. This enhancement in stability may be demonstrated for the linear convection problem through Von Neumann methods. The key point appears to be the approximation of the time derivative term in the convection equation. For time-centered schemes the fundamental temporal difference may be expanded in a Taylor series that includes an infinite number of odd time derivatives and for which only the first derivative is typically retained. In contrast, for the TCT schemes, we have retained the next highest (third) time derivative and evaluated it directly from the original convection equation in a manner similar to that employed by Dukowicz and Ramshaw (1979). In section 2 the various differencing schemes will be applied to the solution of the linear advection equation. For a uniform velocity field the TCT method can also be shown to follow from the Lagrangian method of polynomial fitting as employed by Leith (1965). Pertinent stability results will be presented for this case. In section 3, the influence of a nonuniform velocity field is tested via the standard cone problem—a cone distribution advected by solid-body rotation. The fourth section of the paper will focus attention on applications of

Corresponding author address: Dr. Richard Babarsky, BDM Federal, Inc., 1501 BDM Way, McLean, VA 22102-3204.

these schemes to nonlinear equations. The one-dimensional Burger's equation is analyzed, comparing the applicability of the schemes under consideration, considering various types of errors as well as the total accuracy of the solution for a variety of Courant numbers. Finally a summary is presented in section 5.

2. The one-dimensional linear time-centered scheme—Derivation and stability

For convection-dominated flows it has been maintained that a superior approach for modeling advection processes is based on the method of characteristics (e.g., Raithby 1976), which requires that

$$T(x, t + \Delta t) = T(x - V\Delta t, t)$$

for a region of uniform velocity V. The forward-in-time, finite-difference form of this method was developed by Leith (1965) and Crowley (1968) and subsequently studied by numerous authors. These ''Crowley'' schemes are popular because, at least for the case of uniform flow, they are second-order accurate in time and require only one time level of storage. These advantages diminish somewhat in importance for the case of a nonuniform velocity field, for which the Crowley scheme is usually considered to be first-order accurate in time, and for multidimensional flows, where a ''time splitting'' form in which one full time step is divided into successive time steps in orthogonal directions is required to avoid instabilities. Such instabilities may also be circumvented by replacing the simultaneous application of one-dimensional operators by a form that includes approximations to the cross-space-derivative terms (Smolarkiewicz 1982). Douglas and Russell (1982) have incorporated characteristics in both finite-element-based and finite-difference-based advection schemes to derive the modified method of characteristics technique (MMOC), which yields much smaller time truncation errors than standard methods.

The schemes described above fall into the general class of Lax–Wendroff approximations in which the temporal derivative in the advection equation [see Eq. (1)] is approximated by forward-in-time differencing and the second-order (temporal) derivative appearing in the truncation error is converted to a spatial derivative by virtue of the original equation. For the case of a uniform velocity field this approach is equivalent to expanding $T(x - V\Delta t, t)$ in a Taylor series of arbitrary accuracy. Leapfrog schemes are usually associated with the independent spatial differencing of the flux terms in Eq. (1) to a desired order of accuracy (see Haltiner and Williams 1980) in contrast to the Lax–Wendroff approach. In what follows we shall introduce a class of time-centered schemes by application of the advection characteristic approach. This may be shown to be equivalent to combining forward-time and backward-time Taylor series expansions, including time derivatives of third-order that are evaluated from the governing partial differential equation (we denote such schemes as TCT). This approach results in a scheme which achieves fourth-order accuracy in time and space. Procedures of this type have been used in a forward-in-time context where time derivatives of second order have been retained (see Dukowicz and Ramshaw 1979) and in a finite element context (Donea 1984). Our motivation in taking this approach was to combine the well-established advantages of time-centered differencing (increased temporal accuracy and neutral stability) with the desirable property of point-to-point data transfer that is characteristic of convection-dominated flows and is embodied in Crowley-type schemes. A further advantage, however, is the considerably expanded stability range. Since the TCT schemes represent a direct alternative to the leapfrog methods, popular in large-scale numerical models, a primary objective is the direct comparison of the performance of our hybrid scheme with leapfrog schemes in both linear and nonlinear advection. In this study the effects of features such as cross-space terms and Smolarkiewicz-type modifications to the first partial derivatives will be investigated. Although time-centered schemes do not suffer the long-wave instabilities associated with combined (simultaneous) 1D Crowley operators in multidimensional flows, including cross-space derivative terms will be shown to significantly expand the stability range compared with leapfrog. Moreover, applying Taylor expansions in several dimensions requires essentially one-half the computations in the context of time-centered differencing.

a. Derivation

The equation to be solved is the ''color'' equation describing the advection of a nondiffusive quantity T in a flow field:

$$\frac{\partial T}{\partial t} + \mathbf{v}\cdot\nabla T = 0. \tag{1}$$

Consider the one-dimensional, uniform-velocity case described by the advection equation

$$\frac{\partial T}{\partial t} + u\frac{\partial T}{\partial x} = 0. \tag{2}$$

Using the advection characteristic approach, we begin with the methodology of polynomial fitting, although one could equally well apply Taylor series expansions. Figure 1 shows two characteristic paths in space and time of material points that are at positions x_j at time t^{n+1} and time t^{n-1}, respectively. At time t^n the former point was at position $x_* = x^j - u\Delta t$ and if we know the value of $T = T^n_*$ at time t^n, we can set

$$T^{n+1}_j = T^n_*.$$

However, at time t^n we only know values of T at mesh points x_{j-1}, x_j and x_{j+1}, etc. and hence we must employ an interpolation scheme to determine T^n_*. Similarly,

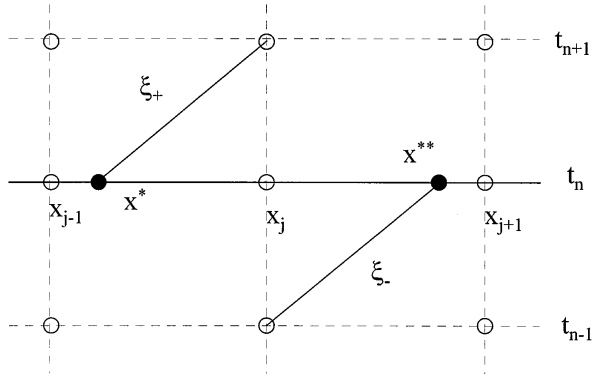

FIG. 1. Advection characteristic diagram.

$$T_j^{n-1} = T_{**}^n,$$

where $x_{**} = x_j + u\Delta t$ and T_{**}^n must be again determined by polynomial interpolation. Assuming a uniformly spaced mesh of interval Δx, for a quadratic interpolating scheme utilizing, T_{j-1}^n, T_j^n, T_{j+1}^n, third-order-accurate approximations in space are given by

$$T_j^{n+1} = T_*^n = T_{j-1}^n \frac{\alpha(\alpha + 1)}{2} + T_j^n(1 - \alpha^2) + T_{j+1}^n \frac{\alpha(\alpha - 1)}{2} + O(\Delta x^3)$$

and

$$T_j^{n-1} = T_{**}^n = T_{j-1}^n \frac{\alpha(\alpha - 1)}{2} + T_j^n(1 - \alpha^2) + T_{j+1}^n \frac{\alpha(1 + \alpha)}{2} + O(\Delta x^3),$$

where the Courant number α is defined as $u\Delta t/\Delta x$.

These expressions may be subtracted to yield a centered-in-time difference scheme (referred to as LF2):

$$T_j^{n+1} = T_j^{n-1} - \alpha(T_{j+1}^n - T_{j-1}^n), \tag{3}$$

which may be recognized as the standard second-order "leapfrog" scheme (see Haltiner and Williams 1980). Considering Taylor series expansions in space and time about (x_j, t^n) yields the result

$$\frac{\partial T}{\partial t} + u\frac{\partial T}{\partial x} + +O(\Delta x^2) + O(\Delta t^2) = \frac{T_j^{n+1} - T_j^{n-1}}{2\Delta t} + u\frac{T_{j+1}^n - T_{j-1}^n}{2\Delta x};$$

that is, this scheme is second-order accurate in time and space.

One may in principle fit a Lagrange polynomial of arbitrary degree to an increasingly larger set of data points. We shall, however, derive the fourth-order extension to Eq. (3) and therefore interpolate T_*^n and T_{**}^n over the values T_{j-2}^n, T_{j-1}^n, T_j^n, T_{j+1}^n, and T_{j+2}^n. Application of this method results in the following difference equation (referred to as the fourth-order "time-centered Taylor" scheme TCT4):

$$T_j^{n+1} = T_j^{n-1} + \frac{\alpha}{6}(-T_{j-2}^n + 8T_{j-1}^n - 8T_{j+1}^n + T_{j+2}^n) + \frac{\alpha^3}{6}(T_{j-2}^n - 2T_{j-1}^n + 2T_{j+1}^n - T_{j+2}^n), \tag{4}$$

which is $O(\Delta x^4) + O(\Delta x^2\,\Delta t^2) + O(\Delta t^4) = O(\Delta x^4) + O(\Delta t^4)$ accurate for a uniform velocity field and $O(\Delta x^4) + O(\Delta x^2\,\Delta t^2) + O(\Delta t^2)$ accurate for an arbitrary velocity field according to this analysis.

Spatial truncation errors of equivalent order result from retaining only the first two terms on the right-hand side of Eq. (4) since the neglected term is equal to $1/6\,\Delta t^3\,(\partial^3 T/\partial t^3)(x_j, t^n) + O(\Delta t^3\,\Delta x^2)$. This yields a simpler fourth-order in space, second-order in time, space-centered scheme for the advection equation (referred to as LF4):

$$T_j^{n+1} = T_j^{n-1} + \frac{\alpha}{6}(-T_{j-2}^n + 8T_{j-1}^n - 8T_{j+1}^n + T_{j+2}^n). \tag{5}$$

Following Crowley (1968), the conservation form of the one-dimensional advection equation, assuming negligible divergence, is

$$\frac{\partial T}{\partial t} = -\frac{\partial F}{\partial x} \tag{6}$$

for $F = uT$. The above results (3) and (4) may also be obtained by Taylor series expansions; first in time and then in space. Consider a semidiscretization of Eq. (6) where we leave the spatial variable x continuous and discretize only the time to obtain a centered, second-order-in-time scheme

$$\frac{T_j^{n+1} - T_j^{n-1}}{2\Delta t} = -\frac{\partial F}{\partial x}.$$

If one replaces the right-hand side by a second-order-accurate centered space approximation, we obtain the classic leapfrog scheme in its conservative form, which reduces to Eq. (3) for the case of uniform velocity u. To produce more accurate temporal differencing, we may proceed as follows: develop third-order-accurate Taylor series expansions, which yield

$$\left(\frac{\partial T}{\partial t}\right)^n = \frac{T^{n+1} - T^{n-1}}{2\Delta t} - \frac{\Delta t^2}{6}\left(\frac{\partial^3 T}{\partial t^3}\right)^n + O(\Delta t^4). \tag{7}$$

For a velocity field that varies slowly in time, the original equation (6) is now used to replace the third-order time derivative in terms of space derivatives as follows:

$$\frac{\partial^3 T}{\partial t^3} = -\frac{\partial}{\partial x}\left\{u\frac{\partial}{\partial x}\left[u\frac{\partial}{\partial x}(F)\right]\right\}. \tag{8}$$

Combining Eqs. (7) and (8), the original Eq. (6) may

be approximated by the semidiscrete equation at time level n:

$$\frac{T^{n+1} - T^{n-1}}{2\Delta t} = \left(\frac{\partial \mathcal{F}}{\partial x}\right)^n, \tag{9}$$

where

$$\mathcal{F} = uT + u\frac{\partial}{\partial x}\left(u\frac{\partial F}{\partial x}\right)\frac{\Delta t^2}{6}$$
$$= u\left[T + \frac{\partial}{\partial x}\left(u\frac{\partial F}{\partial x}\right)\frac{\Delta t^2}{6}\right]$$

represents a modified convective flux [although it actually contains part of the difference approximation to $(\partial T/\partial t)^n$]. This interpretation is useful if one wishes the difference equations to satisfy the integral balance implied by the differential system. Moreover, since Eq. (9) has been derived in divergence form it lends itself naturally to the construction of conservative difference equations.

If we make the further assumption that u = const, we obtain

$$\frac{\partial^3 T}{\partial t^3} = -u^3\frac{\partial^3 T}{\partial x^3},$$

which results in the following semidiscrete equation at time level n:

$$\frac{T^{n+1} - T^{n-1}}{2\Delta t} + \frac{\Delta t^2}{6}u^3\left(\frac{\partial^3 T}{\partial x^3}\right)^n = -u\left(\frac{\partial T}{\partial x}\right)^n. \tag{10}$$

Hence,

$$T^{n+1} - T^{n-1} = -2u\Delta t\left(\frac{\partial T}{\partial x}\right)^n - \frac{\Delta t^3}{3}u^3\left(\frac{\partial^3 T}{\partial x^3}\right)^n,$$

which may also be obtained directly from a Taylor expansion. To obtain fourth-order accuracy in space as well as time, we introduce higher-order approximations for the first-order spatial derivative, yielding

$$T_j^{n+1} = T_j^{n-1} + \frac{\alpha}{6}(-T_{j-2}^n + 8T_{j-1}^n - 8T_{j+1}^n + T_{j+2}^n)$$
$$+ \frac{\alpha^3}{6}(T_{j-2}^n - 2T_{j-1}^n + 2T_{j+1}^n - T_{j+2}^n),$$

which is the TCT4 scheme. If one applies second-order differencing to all spatial derivatives, we obtain the second-order TCT2 scheme:

$$T_j^{n+1} = T_j^{n-1} + \alpha(-T_{j+1}^n + T_{j-1}^n)$$
$$+ \frac{\alpha^3}{6}(T_{j-2}^n - 2T_{j-1}^n + 2T_{j+1}^n - T_{j+2}^n). \tag{11}$$

b. Stability

The stability characteristics of the second-order leapfrog scheme are well known (see Haltiner and Williams 1980). We shall be interested in scrutinizing the influence of higher-order approximations in the context of centered-in-time differencing. In particular the application of advection characteristic (or equivalently TCT) methods versus traditional leapfrog methods will be studied. These schemes are characterized by an expanded spatial stencil relative to LF2, hence Von Neumann methods will be applied for the sake of simplicity. This approach precludes a comprehensive treatment of boundary conditions that would require higher-order GKS theory (see Strikwerda 1989).

TABLE 1. Form of σ for one-dimensional finite-difference advection schemes tested.

Scheme	Expression for σ
LF2	$\alpha \sin(\mu\Delta x)$
LF4	$\frac{\alpha \sin(\mu\Delta x)}{3}[4 - \cos(\mu\Delta x)]$
TCT2	$\frac{\alpha \sin(\mu\Delta x)}{3}\{3 + \alpha^2[\cos(\mu\Delta x) - 1]\}$
TCT4	$\frac{\alpha \sin(\mu\Delta x)}{3}\{4 - \cos(\mu\Delta x) + \alpha^2[\cos(\mu\Delta x) - 1]\}$

Consider a harmonic solution to the advection equation

$$T(x, t) = e^{i\mu(x-ut)} = T(x, 0)e^{-i\mu ut},$$

where the initial distribution $T(x, 0)$ is simply translated a distance ut in time t and after a time Δt the solution has phase angle $\phi = -\mu u\Delta t$. Solutions to the difference schemes derived above that take into account the harmonic initial condition have the form

$$T_j^n = r^n e^{ij\mu\Delta x}, \tag{12}$$

where r represents the eigenvalue of the given difference operator. For each of the centered-in-time difference equations above, substituting Eq. (12) for T_j^n yields an eigenvalue equation of the form

$$r^2 + 2i\sigma r - 1 = 0, \tag{13}$$

where σ depends on α and $\mu\Delta x$ and varies according to which scheme is being considered. The specific expressions for σ, for the methods developed above, are displayed in Table 1. Solving the eigenvalue equation (13) gives

$$r = \pm(1 - \sigma^2)^{1/2} - i\sigma.$$

Thus, such time-centered methods possess neutral stability ($|r| = 1$) provided

$$\sigma^2 \leq 1$$

and are computationally unstable if

$$\sigma^2 > 1.$$

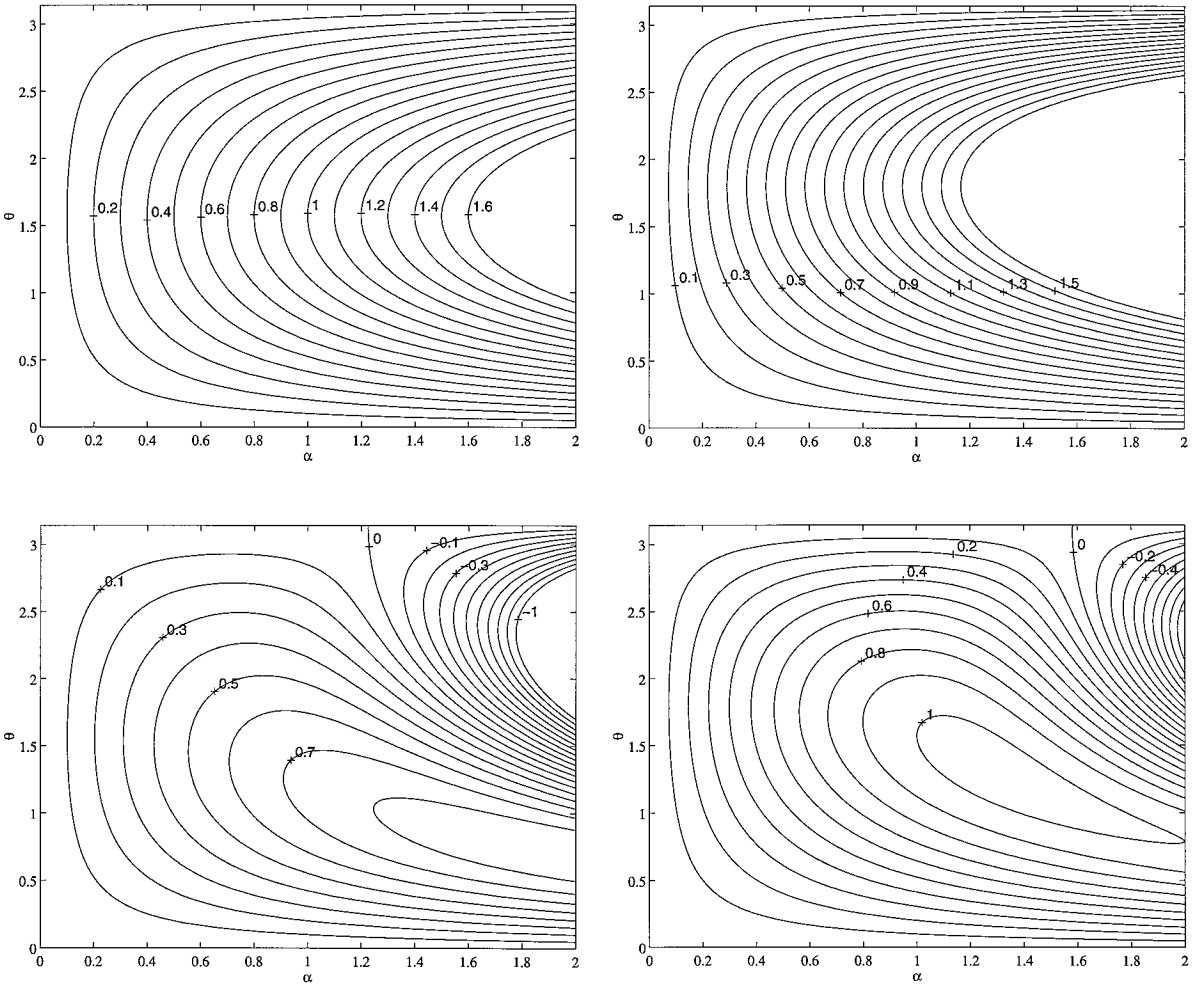

FIG. 2. Level lines of σ for different time-centered schemes as a function of α and θ (labels from upper left to lower right): (a) LF2, (b) LF4, (c) TCT2, and (d) TCT4.

The numerical phase angle in time Δt for the time-centered methods developed above is

$$\phi_{\text{num}} = \arg(r) = \sin^{-1}\left[\frac{\text{Im}(r)}{|r|}\right] = -\sin^{-1}(\sigma)$$

and, in general, $\phi_{\text{num}} \neq \phi = -\mu u \Delta t = -\alpha\mu\Delta x$. Thus, the relative phase error during a time increment Δt is

$$\frac{\Delta\phi}{\phi} = \frac{\phi - \phi_{\text{num}}}{\phi} = 1 - \frac{\phi_{\text{num}}}{-\alpha\mu\Delta x}.$$

In order to examine the relationship of the solution obtained by difference approximations to the analytic solution, contour plots of σ and relative phase error ($\Delta\phi/\phi$), as functions of α and $\mu\Delta x$, have been constructed. Figures 2a–d present level lines of σ for the various schemes to be considered. Since values of $|\sigma| \leq 1$ cover numerically stable regions it is seen in Fig. 2a that the second-order leapfrog scheme (3) is stable for all wavenumbers if $|\alpha| \leq 1$ with the maximum amplitude corresponding to $\theta = \mu\Delta x = \pi/2$. Figure 2b presents the fourth-order leapfrog scheme (5), which is stable if $|\alpha| \leq 6(9 + 24\sqrt{6})^{-1/2} \approx 0.73$ with the unstable mode shifted toward the shorter wavelengths $\mu\Delta x = \arccos(1 - \sqrt{6}/2) \approx 0.57\pi$. Application of the fourth-order advection characteristic (TCT) methods appears to enhance stability relative to the space-centered leapfrog schemes. From Fig. 2d we see that, for the fourth-order form (4), stability is insured for all θ provided $|\alpha| \leq 1$ (with maximum amplitude occurring at $\mu\Delta x = \pi/2$), which compares with the second-order leapfrog scheme (3). Moreover, the region of instability, which is significantly contracted, is shifted away from the shorter wavelength (higher wavenumber) modes. As for the TCT2 form (11) displayed in Fig. 2c, the maximum Courant number compatible with stability is further increased to 1.77 and the unstable wavelengths are shortened to a smaller region centered at $\mu\Delta x \approx 0.72\pi$.

Figures 3a–d are contour plots of the relative phase error ($\Delta\phi/\phi$) computed for each of the schemes dis-

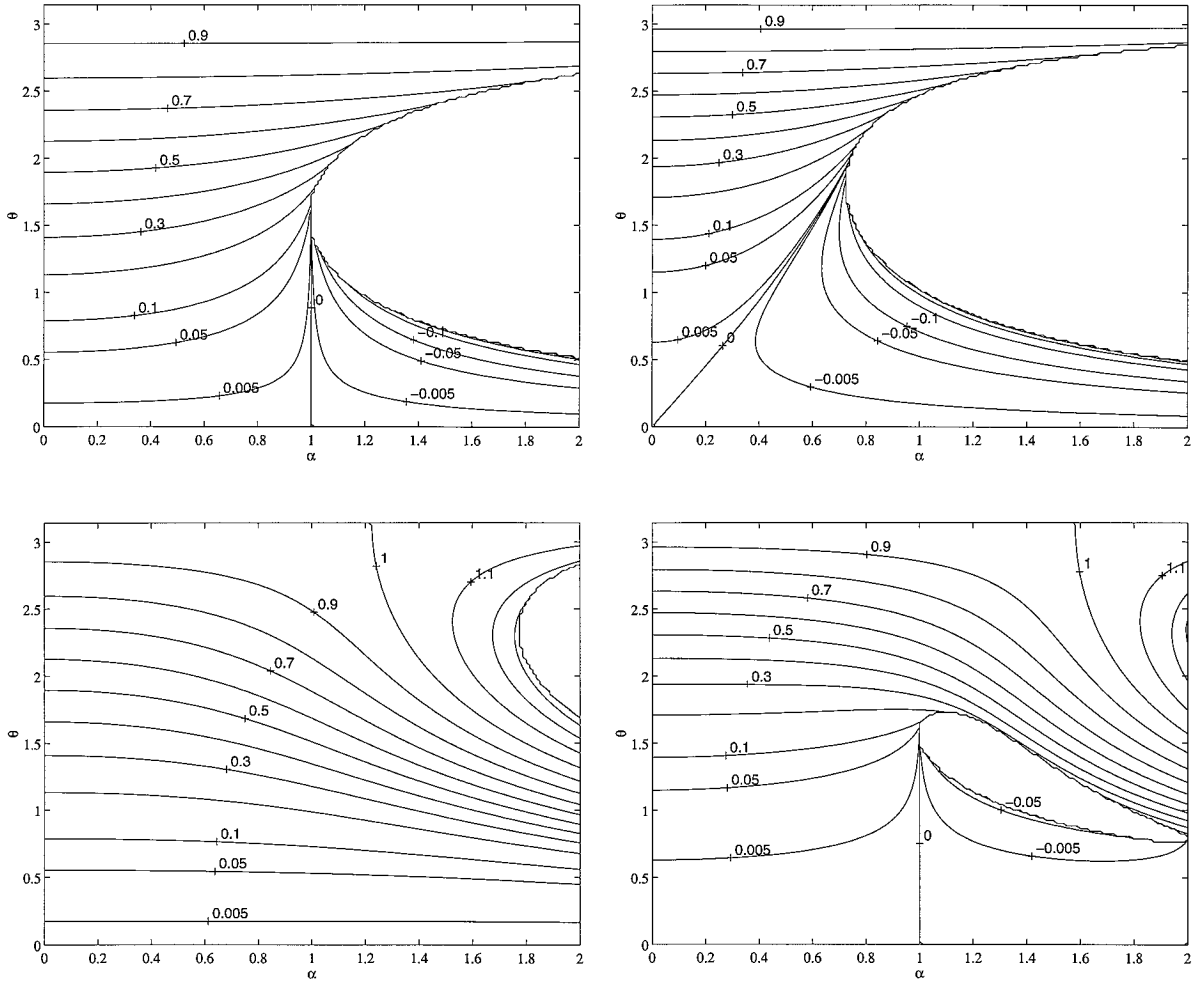

FIG. 3. Level lines of $\Delta\phi/\phi$ for different time-centered schemes function of α and θ (labels from upper left to lower right): (a) LF2, (b) LF4, (c) TCT2, and (d) TCT4.

cussed above. It is seen that for these schemes, in their respective stable regions, the values along the contours (which are between -0.1 and 1.2) indicate that waves in the numerical solution generally lag behind the corresponding analytical solutions. These figures all exhibit similar characteristics in their corresponding stable regions. For a fixed value of α, relative phase error increases from 0 to a maximum of 1 as $\mu\Delta x$ increases from 0 (infinite wavelength) to π ($2\Delta x$ wavelength). This latter value is the highest wavenumber a given mesh can support and this wave has a zero phase velocity, that is, it is stationary. For a given wavenumber relative phase error is weakly dependent on the Courant number with the leapfrog schemes showing slight improvement with α (up to the stability limit) and the advection characteristic methods exhibiting a mild deterioration. This tendency is somewhat more critical for the TCT2 scheme since its region of stability extends far beyond those of the others. However, the primary distinction is between the performance of the second-order schemes and the fourth-order schemes (as emphasized by Fromm 1968). Comparison of Figs. 3a and 3b shows that fourth-order leapfrog considerably improves the phase behavior of long-wavelength modes relative to the second-order scheme (contours are clearly squeezed toward the stationary mode $\mu\Delta x = \pi$ with a resulting broadening of the near-zero-phase-error region). Comparison of Fig. 3d with Fig. 3b shows that the fourth-order TCT method possesses very similar phase properties to that of fourth-order leapfrog except for a triangular region of leading phase error for $|\alpha| < 0.72$ in the case of LF4, Fig. 3b (in the stable regime). The advection TCT form exhibits no such anomalous region, hence positive phase characteristics extend throughout its stability region.

3. Linear advection in two dimensions

Leith (1965) and others have demonstrated that the second-order, forward-in-time numerical approximation

of two-dimensional advection is unstable if one-dimensional operators are applied simultaneously. The corresponding question in the context of centered-in-time differencing will be considered in this section.

Anticipating stability problems when combining one-dimensional operators for modeling two-dimensional advection, we take an approach by multivariate Taylor approximations. Along an advection characteristic, we have

$$T(x, y, t + \Delta t) = T(x - u\Delta t, y - v\Delta t, t) \quad (14)$$

and

$$T(x, y, t - \Delta t) = T(x + u\Delta t, y + v\Delta t, t). \quad (15)$$

Expanding $T(x_j, y_k, t^{n\pm1})$ about (x_j, y_k, t^n) to second order and subtracting the resulting expressions gives

$$T_{jk}^{n+1} = T_{jk}^{n-1} - 2u\Delta t\frac{\partial}{\partial x}T_{jk}^n - 2v\Delta t\frac{\partial}{\partial y}T_{jk}^n + O(\Delta t^3);$$

thus, to second order, no cross-derivative terms appear in the corresponding Taylor expansion; including the second-order-accurate approximation of the first partial derivatives, for example,

$$\frac{\partial}{\partial x}T_{jk}^n = \frac{T_{j+1k}^n - T_{j-1k}^n}{2\Delta x} + O(\Delta x^2),$$

and retaining terms to like order yields a simple combination of one-dimensional operators

$$T_{jk}^{n+1} = T_{jk}^{n-1} - \alpha\,(T_{j+1k}^n - T_{j-1k}^n) - \beta\,(T_{jk+1}^n - T_{jk-1}^n), \quad (16)$$

where $\alpha = u\,\Delta t/\Delta x$ and $\beta = v\,\Delta t/\Delta x$ and these parameters are specified without indices for the case of uniform velocity (note that a nonuniform velocity field would require a staggered grid representation). Smolarkiewicz (1982) suggests that, for the case of the forward-in-time advection scheme, stability is enhanced by replacing the original second-order-accurate approximation to the first spatial partial derivative with one that includes information about the dimensionally of the field, for example,

$$\frac{\partial}{\partial x}T_{jk}^n = \frac{0.5(T_{j+1k+1}^n + T_{j+1k-1}^n) - 0.5(T_{j-1k+1}^n + T_{j-1k-1}^n)}{2\Delta x} + O(\Delta x^2).$$

This modification leads, in combination with central time-differencing, to a second-order finite-difference algorithm for Eq. (1) in the form

$$\begin{aligned} T_{jk}^{n+1} = T_{jk}^{n-1} &- \alpha[0.5(T_{j+1k+1}^n + T_{j+1k-1}^n) \\ &- 0.5(T_{j-1k+1}^n + T_{j-1k-1}^n)] \\ &- \beta[0.5(T_{j+1k+1}^n + T_{j-1k+1}^n) \\ &- 0.5(T_{j+1k-1}^n + T_{j-1k-1}^n)]. \end{aligned} \quad (17)$$

Next we derive a two-dimensional, fourth-order scheme by combining fourth-order Taylor expansions for the right-hand sides of Eqs. (14) and (15). This yields

$$\begin{aligned} T_{jk}^{n+1} = T_{jk}^{n-1} &- 2u\Delta t\frac{\partial}{\partial x}T_{jk}^n - 2v\Delta t\frac{\partial}{\partial y}T_{jk}^n \\ &- 2\frac{u^3\Delta t^3}{6}\frac{\partial^3}{\partial x^3}T_{jk}^n - u^2v\Delta t^3\frac{\partial^3}{\partial x^2\partial y}T_{jk}^n \\ &- uv^2\Delta t^3\frac{\partial^3}{\partial x\partial y^2}T_{jk}^n - 2\frac{v^3\Delta t^3}{6}\frac{\partial^3}{\partial y^3}T_{jk}^n \\ &+ O(\Delta t^5). \end{aligned} \quad (18)$$

Replacing the first-order derivatives in Eq. (18) with fourth-order-accurate approximations and all remaining higher-order derivatives with second-order-accurate expressions leads to the following form:

$$\begin{aligned} T_{jk}^{n+1} = T_{jk}^{n-1} &+ \frac{\alpha}{6}(-T_{j-2k}^n + 8T_{j-1k}^n - 8T_{j+1k}^n + T_{j+2k}^n) + \frac{\beta}{6}(-T_{jk-2}^n + 8T_{jk-1}^n - 8T_{jk+1}^n + T_{jk+2}^n) \\ &+ \frac{\alpha^3}{6}(T_{j-2k}^n - 2T_{j-1k}^n + 2T_{j+1k}^n - T_{j+2k}^n) \\ &- \frac{\alpha^2\beta}{2}[(T_{j+1k+1}^n - 2T_{jk+1}^n + T_{j-1k+1}^n) - (T_{j+1k-1}^n - 2T_{jk-1}^n + T_{j-1k-1}^n)] \\ &- \frac{\alpha\beta^2}{2}[(T_{j+1k+1}^n - 2T_{j+1k}^n + T_{j+1k-1}^n) - (T_{j-1k+1}^n - 2T_{j-1k}^n + T_{j-1k-1}^n)] \\ &+ \frac{\beta^3}{6}(T_{jk-2}^n - 2T_{jk-1}^n + 2T_{jk+1}^n - T_{jk+2}^n), \end{aligned} \quad (19)$$

which is a fourth-order scheme. We obtain the two-dimensional TCT2 scheme by applying second-order-accurate approximations to all spatial derivatives in Eq. (18):

$$T_{jk}^{n+1} = T_{jk}^{n-1} - \alpha(T_{j+1k}^{n} - T_{j-1k}^{n}) - \beta(T_{jk+1}^{n} - T_{jk-1}^{n}) + \frac{\alpha^3}{6}(T_{j-2k}^{n} - 2T_{j-1k}^{n} + 2T_{j+1k}^{n} - T_{j+2k}^{n})$$
$$- \frac{\alpha^2\beta}{2}[(T_{j+1k+1}^{n} - 2T_{jk+1}^{n} + T_{j-1k+1}^{n}) - (T_{j+1k-1}^{n} - 2T_{jk-1}^{n} + T_{j-1k-1}^{n})]$$
$$- \frac{\alpha\beta^2}{2}[(T_{j+1k+1}^{n} - 2T_{j+1k}^{n} + T_{j+1k-1}^{n}) - (T_{j-1k+1}^{n} - 2T_{j-1k}^{n} + T_{j-1k-1}^{n})]$$
$$+ \frac{\beta^3}{6}(T_{jk-2}^{n} - 2T_{jk-1}^{n} + 2T_{jk+1}^{n} - T_{jk+2}^{n}). \quad (20)$$

If we average over neighboring points (in a plane) when approximating the first spatial partial derivatives (per Smolarkiewicz), we obtain [as an alternative to Eq. (19)]

$$T_{jk}^{n+1} = T_{jk}^{n-1} + \frac{\alpha}{6}[-0.5(T_{j-2k-1}^{n} + T_{j-2k+1}^{n}) + 8(0.5)(T_{j-1k-1}^{n} + T_{j-1k+1}^{n})$$
$$-8(0.5)(T_{j+1k-1}^{n} + T_{j+1k+1}^{n}) + 0.5(T_{j+2k-1}^{n} + T_{j+2k+1}^{n})]$$
$$+ \frac{\beta}{6}[-0.5(T_{j-1k-2}^{n} + T_{j+1k-2}^{n}) + 8(0.5)(T_{j-1k-1}^{n} + T_{j+1k-1}^{n})$$
$$-8(0.5)(T_{j-1k+1}^{n} + T_{j+1k+1}^{n}) + 0.5(T_{j-1k+2}^{n} + T_{j+1k+2}^{n})]$$
$$+ \frac{\alpha^3}{6}(T_{j-2k}^{n} - 2T_{j-1k}^{n} + 2T_{j+1k}^{n} - T_{j+2k}^{n})$$
$$- \frac{\alpha^2\beta}{2}[(T_{j+1k+1}^{n} - 2T_{jk+1}^{n} + T_{j-1k+1}^{n}) - (T_{j+1k-1} - 2T_{jk-1}^{n} + T_{j-1k-1}^{n})]$$
$$- \frac{\alpha\beta^2}{2}[(T_{j+1k+1}^{n} - 2T_{j+1k}^{n} + T_{j+1k-1}^{n}) - (T_{j-1k+1} - 2T_{j-1k}^{n} + T_{j-1k-1}^{n})]$$
$$+ \frac{\beta^3}{6}(T_{jk-2}^{n} - 2T_{jk-1}^{n} + 2T_{jk+1}^{n} - T_{jk+2}^{n}). \quad (21)$$

Finally, to test the efficacy of our approach we will consider the standard nonconservative fourth-order, space-centered approximation:

$$T_{jk}^{n+1} = T_{jk}^{n-1} + \frac{\alpha}{6}(-T_{j-2k}^{n} + 8T_{j-1k}^{n} - 8T_{j+1k}^{n} + T_{j+2k}^{n})$$
$$+ \frac{\beta}{6}(-T_{jk-2}^{n} + 8T_{jk-2}^{n} - 8T_{jk+1}^{n} + T_{jk+2}^{n}). \quad (22)$$

In order to easily reference the various difference schemes being considered in this paper we will designate the two-dimensional schemes defined by Eqs. (16), (17), (19), (20), (21), and (22) by LF2, SM2, TCT4, TCT2, TCT4Sm, and LF4, respectively. Although several of these labels have been previously used to specify one-dimensional difference schemes, we assert that the context will obviate any ambiguity.

a. Flux conservative form

As in the one-dimensional case, one may demonstrate the equivalence of the preceding derivation with an approach based on a conservative flux form of Eq. (1). Consider the conservation form of Eq. (1) assuming negligible divergence,

$$\frac{\partial T}{\partial t} + \nabla\cdot\mathbf{F} = 0, \quad (23)$$

where $\mathbf{F} = (T\mathbf{v})$. We proceed by considering the temporal differencing separately from the spatial differencing. Accordingly, we leave the spatial variable continuous and discretize only the time to obtain the centered temporal difference approximation to Eq. (23):

$$\frac{T^{n+1} - T^{n-1}}{2\Delta t} + (\nabla\cdot\mathbf{F})^n = 0. \quad (24)$$

A numerical algorithm can be described as follows. Develop a third-order Taylor series expansion in time about t^n in the form

$$T^{n+1} = T^n + \Delta t\left(\frac{\partial T}{\partial t}\right)^n + \frac{\Delta t^2}{2}\left(\frac{\partial^2 T}{\partial t^2}\right)^n + \frac{\Delta t^3}{6}\left(\frac{\partial^3 T}{\partial t^3}\right)^n + \cdots.$$

Similarly,

$$T^{n-1} = T^n - \Delta t\left(\frac{\partial T}{\partial t}\right)^n + \frac{\Delta t^2}{2}\left(\frac{\partial^2 T}{\partial t^2}\right)^n - \frac{\Delta t^3}{6}\left(\frac{\partial^3 T}{\partial t^3}\right)^n + \cdots.$$

Thus we obtain

$$\frac{T^{n+1} - T^{n-1}}{2\Delta t} = \left(\frac{\partial T}{\partial t}\right)^n + \frac{\Delta t^2}{6}\left(\frac{\partial^3 T}{\partial t^3}\right)^n + O(\Delta t^4).$$

Using Eq. (23) and assuming a slowly varying velocity field, we may estimate the time truncation error as follows:

$$\frac{T^{n+1} - T^{n-1}}{2\Delta t} = \left(\frac{\partial T}{\partial t}\right)^n - \frac{\Delta t^2}{6}\nabla\cdot\{\mathbf{vv}\cdot\nabla[\nabla\cdot(T\mathbf{v})] - \nabla\cdot(T\mathbf{v})\mathbf{v}(\nabla\cdot\mathbf{v})\} + O(\Delta t^4). \quad (25)$$

Now if one applies reasoning consistent with Dukowicz and Ramshaw (1979), the term of crucial importance should be proportional to **v** (rather than derivatives of **v**) since enhanced stability characteristics will be shown to persist even when **v** is independent of position and time. Hence, neglecting terms of the form $\nabla\cdot\mathbf{v}$ or $\partial\mathbf{v}/\partial t$, we replace the expression in braces by

$$\mathbf{vv}\cdot(\mathbf{v}\cdot\nabla)\nabla T;$$

that is, we approximate $(\partial T/\partial t)^n$ by

$$\frac{T^{n+1} - T^{n-1}}{2\Delta t} + \frac{\Delta t^2}{6}\nabla\cdot[\mathbf{vv}\cdot(\mathbf{v}\cdot\nabla)\nabla T].$$

The difference scheme then becomes, instead of Eq. (25), a second-order approximation (in time) overall but fourth order in the most important effect. Thus, analogous to Eq. (9), we have

$$\frac{T^{n+1} - T^{n-1}}{2\Delta t} + \nabla\cdot(T\mathbf{v})^n = -\frac{\Delta t^2}{6}\nabla\cdot[\mathbf{vv}\cdot(\mathbf{v}\cdot\nabla)\nabla T]^n,$$

where $\mathbf{vv} = \mathbf{vv}^{\mathrm{T}}$ is a second-order tensor (see Bird et al. 1960). This can also be placed in a conservative flux form:

$$\frac{T^{n+1} - T^{n-1}}{2\Delta t} = -\nabla\cdot\mathcal{F}^n, \quad (26)$$

where

$$\mathcal{F}^n = T\mathbf{v} + \frac{\Delta t^2}{6}\mathbf{vv}\cdot(\mathbf{v}\cdot\nabla)\nabla T.$$

The two-dimensional formulation in Cartesian coordinates yields, in component form,

$$\mathcal{F}_1^n = uT + \frac{\Delta t^2}{6}\left\{u^3\frac{\partial^2 T}{\partial x^2} + 2vu^2\frac{\partial^2 T}{\partial x\partial y} + uv^2\frac{\partial^2 T}{\partial y^2}\right\} \quad (27)$$

and

$$\mathcal{F}_2^n = vT + \frac{\Delta t^2}{6}\left\{u^2v\frac{\partial^2 T}{\partial x^2} + 2uv^2\frac{\partial^2 T}{\partial x\partial y} + v^3\frac{\partial^2 T}{\partial y^2}\right\}. \quad (28)$$

Replacing the derivatives in Eqs. (27) and (28) with second-order-accurate approximation leads to the following discretized expressions for the modified horizontal flux component at the *u* stagger points and the modified vertical flux component at the *v* stagger points:

$$\mathcal{F}_1 = u_{jk}\frac{(T_{j+1k} + T_{j,k})}{2} + \frac{\Delta t^2}{6}\left\{u_{jk}^3\frac{(T_{j+2k} - T_{j+1k} - T_{jk} + T_{j-1k})}{2\Delta x^2} + 2u_{jk}^2\frac{(v_{jk} + v_{j+1k} + v_{jk-1} + v_{j+1k-1})}{4}\frac{(T_{j+1k+1} - T_{jk+1} - T_{j+1k-1} + T_{jk-1})}{2\Delta x\Delta y} + 2u_{jk}\frac{(v_{jk} + v_{j+1k} + v_{jk-1} + v_{j+1k-1})^2}{4}\frac{[T_{jk+1} + T_{j+1k+1} - 2(T_{jk} ++ T_{j+1k}) + T_{jk-1} + T_{j+1k-1}]}{2\Delta y^2}\right\}$$

$$\mathcal{F}_2 = v_{jk}\frac{(T_{jk+1} + T_{jk})}{2} + \frac{\Delta t^2}{6}\left\{v_{jk}^3\frac{(T_{jk+2} - T_{jk+1} - T_{jk} + T_{jk-1})}{2\Delta y^2} + 2v_{jk}^2\frac{(u_{j-1k} + u_{jk} + u_{j-1k+1} + u_{jk+1})}{4}\frac{(T_{j+1k+1} - T_{j-1k+1} - T_{j+1k} + T_{j-1k})}{2\Delta x\Delta y} + 2v_{jk}\left(\frac{u_{j-1k} + u_{jk} + u_{j-1k+1} + u_{jk+1}}{4}\right)^2\frac{[T_{j+1k} + T_{j+1k+1} - 2(T_{jk} ++ T_{jk+1}) + T_{j-1k} + T_{j-1k+1}]}{2\Delta x^2}\right\}.$$

TABLE 2. Form of σ for two-dimensional finite-difference advection schemes tested.

Scheme	Expression for σ
LF2	$\alpha \sin(\mu\Delta x) + \beta \sin(\nu\Delta y)$
SM2	$\alpha \sin(\mu\Delta x)\cos(\nu\Delta y) + \beta \sin(\nu\Delta y)\cos(\mu\Delta x)$
TCT2	$\frac{\alpha \sin(\mu\Delta x)}{3}\{3 + a^2[\cos(\mu\Delta x) - 1]\} + \frac{\beta \sin(\nu\Delta y)}{3}\{3 + \beta^2[\cos(\nu\Delta y) - 1]\}$ $-a^2\beta \sin(\nu\Delta y)[1 - \cos(\mu\Delta x)]^3 - \alpha\beta^2 \sin(\mu\Delta x)][1 - \cos(\nu\Delta y)]$
TCT4	$\frac{\alpha \sin(\mu\Delta x)}{3}\{4 - \cos(\mu\Delta x) + \alpha^2[\cos(\mu\Delta x) - 1]\} + \frac{\beta \sin(\nu\Delta y)}{3}\{4 - \cos(\nu\Delta y) + \beta^2[\cos(\nu\Delta y) - 1]\}$ $-\alpha^2\beta \sin(\nu\Delta y)[1 - \cos(\mu\Delta x)]^3 - \alpha\beta^2 \sin(\mu\Delta x)[1 - \cos(\nu\Delta y)]$
TCT4SM	$\frac{\alpha \sin(\mu\Delta x)}{3}\{[4 - \cos(\mu\Delta x)]\cos(\nu\Delta y) + \alpha^2[\cos(\mu\Delta x) - 1] + 3\beta^2[\cos(\nu\Delta y) - 1]\} + \frac{\beta \sin(\nu\Delta y)}{3}$ $\times \{[4 - \cos(\nu\Delta y)]\cos(\nu\Delta x) + \beta^2[\cos(\nu\Delta y) - 1] + 3\alpha^2[\cos(\mu\Delta x) - 1]\}$
LF4	$\frac{\alpha \sin(\mu\Delta x)}{3}[4 - \cos(\mu\Delta x)] + \frac{\beta \sin(\nu\Delta y)}{3}[4 - \cos(\nu\Delta y)]$

Thus Eq. (26) may be approximated by the following scheme:

$$T_{j,k}^{n+1} - T_{j,k}^{n-1} = -2\Delta t\frac{(\mathcal{F}_1^n)_{j,k} - (\mathcal{F}_1^n)_{j-1,k}}{\Delta x} - 2\Delta t\frac{(\mathcal{F}_2^n)_{j,k} - (\mathcal{F}_2^n)_{j,k-1}}{\Delta y}, \quad (29)$$

where, for the case of a uniform velocity field, Eq. (29) reduces to (20). Alternatively, when considering constant velocity, a fourth-order approximation for the advected quantity T leads to Eq. (22).

b. Stability

Wave-type solutions exist for the finite difference approximations to Eq. (1) for uniform flow provided boundary considerations may be neglected. These solutions are of the form

$$T_{jk}^n = r^n e^{i(j\mu\Delta x + k\nu\Delta y)},$$

where $\mu\Delta x$ and $\nu\Delta y$ are the components of the wavenumber in the x and y directions. As with the one-dimensional case r the amplification factor or eigenvalue satisfies a quadratic equation (13) and, hence, neutral stability follows provided $\sigma^2 \leq 1$ and the numerical solution is unstable otherwise.

The relative phase error per time step is given by

$$\frac{\Delta\phi}{\phi} = 1 - \frac{\phi_{\text{num}}}{\phi}.$$

The phase shift ϕ of the true solution is $-(\alpha\mu\Delta x + \beta\nu\Delta y)$, and ϕ_{num}, the numerical phase shift, is given once again by

$$\arg(r) = \sin^{-1}(-\sigma).$$

The stability characteristics of each of the numerical schemes described above is dictated by the parameter σ, where σ depends on the Courant numbers α and β and the wavenumbers $\mu\Delta x$ and $\nu\Delta y$. The specific form of σ for these methods is displayed in Table 2.

We begin by investigating the behavior of σ as a function of α and β. Recall that values of σ such that $|\sigma| \leq 1$ preserve amplitude, while values of σ exceeding 1 in magnitude indicate an unstable mode. Following Fromm (1968) we will restrict our attention to modes satisfying

$$\theta = \mu\Delta x = \nu\Delta y.$$

These symmetrical modes have been identified with maximum instability, and it is assumed that an emphasis on the behavior of crucial short waves will provide a critical view of the linear behavior of the schemes being studied. Moreover, by examining the expressions for σ included in Table 2, we see that for such symmetric modes all schemes exhibit isotropic behavior along the lines $\xi = \alpha + \beta =$ constant.

The results of the linear analysis for each scheme are shown in Figs. 4a–f and Figs. 5a–f. In these figures the quantity of interest, either σ or $\Delta\phi/\phi$, is plotted in (ξ, θ) space with ξ increasing from 0 to 2 rightward along the abscissas and θ increasing from 0 to π upward along the ordinate. Note that in the case of 2Δ wavelength (i.e., $\theta = \pi$) the waves are stationary since each of the expressions in Table 2 has $\sin\theta$ as a factor implying $\sigma \equiv 0$.

Figures 4a,b and 5a,b contrast the well-known stability properties of LF2 and its modified (per Smolarkiewicz) counterpart SM2. The modified scheme is char-

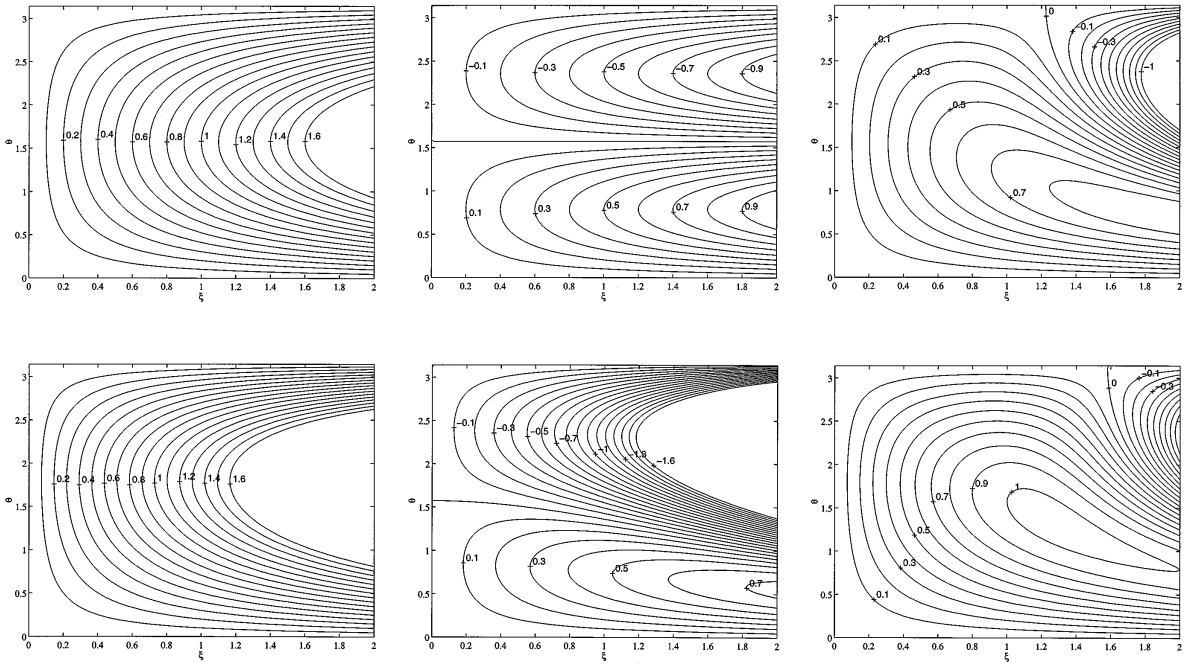

FIG. 4. Level lines of σ for the different two-dimensional, time-centered schemes as a function of $\xi = \alpha + \beta$ and θ (labels from upper left to lower right): (a) LF2, (b) SM2, (c) TCT2, (d) LF4, (e) TCT4SM, and (f) TCT4.

acterized by a substantially expanded stability range, $c = (\alpha^2 + \beta^2)^{1/2} \leq 1.4$ with critical behavior for 8Δ (2, $\pi/4$) and $8\Delta/3$ (2, $3\pi/4$) waves. LF2 is stable for $c \leq 0.71$ with the minimum unstable Courant number occurring for $\theta = \pi/2$. Contrasting these with similar results for Crowley-type (single step, forward-in-time) schemes shows that, in contradistinction with the latter, where stability is limited by longer waves, c passes through a minimum in the short wavelength range.

Although the stability region for SM2 is less restricted

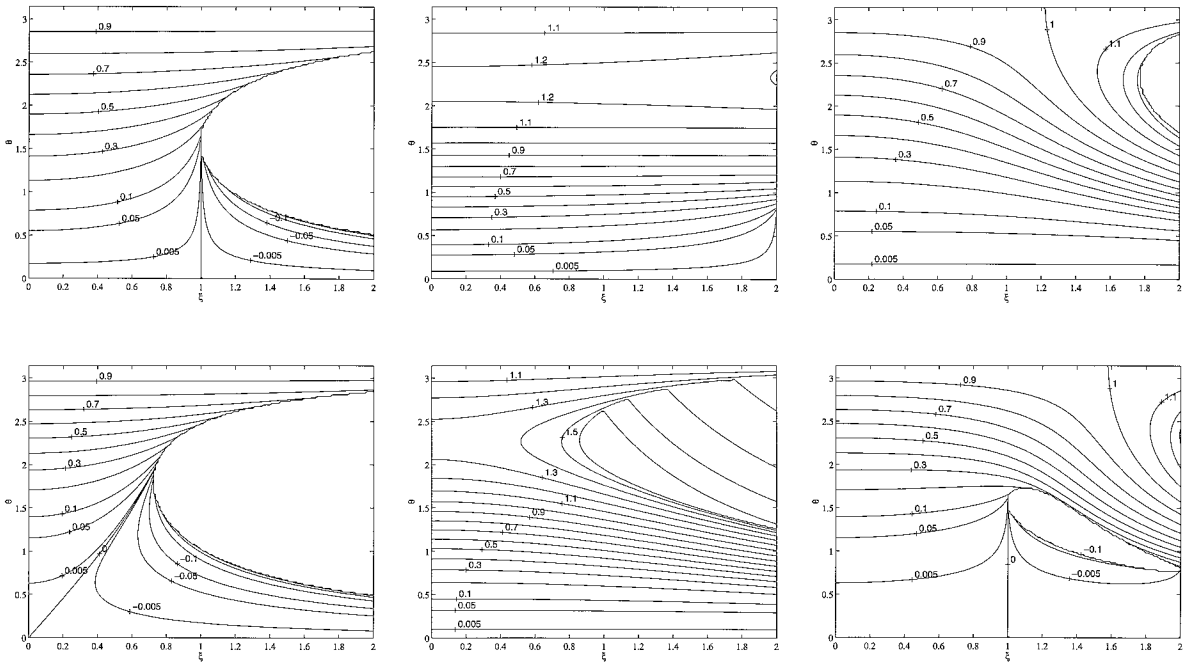

FIG. 5. Level lines $\Delta\phi/\phi$ for the different two-dimensional, time-centered schemes as a function of $\xi = \alpha + \beta$ and θ (labels from upper left to lower right): (a) LF2, (b) SM2, (c) TCT2, (d) LF4, (e) TCT4SM, and (f) TCT4.

than for LF2, Fig. 5b shows the pronounced dispersive phase lag that afflicts this scheme. In fact, one can observe from the appropriate expressions for σ in Table 2 that terms involving $\sin\theta$ in σ_{LF2} are replaced by terms involving $\cos\theta \sin\theta$ in σ_{SM2} and hence for $\pi/2 \leq \theta \leq \pi$ (i.e., short waves for which $\lambda \leq 4\Delta$) the phase velocity of the SM2 numerical solution changes sign while the LF2 solution simply lags the true solution. This means that short-wavelength modes are either stationary or traveling in a direction opposite to that of the actual wave. This feature is particularly damaging for time-centered schemes in which neutral stability throughout a significant range of the α–β plane means that large phase errors will not be compensated for by large-amplitude damping as is the case for Crowley-type schemes (see Smolarkiewicz 1982).

As stated by Fromm (1968), higher-order methods are required in order to significantly improve the phase properties of centered difference schemes. Since all methods being compared possess neutral stability, defining a best method must focus on expanding the stability region and/or reducing dispersion.

Figures 4c–f and 5c–f compare the stability characteristics of the various fourth-order schemes being considered (LF4, TCT4, and TCT4SM), as well as the hybrid TCT2 scheme. The most significant result for these schemes concerns the expanded stability regions achieved by the advection characteristic methods. In particular, the TCT2 algorithm achieves neutral stability in the range $\alpha + \beta \leq 1.82$ or $c = (\alpha^2 + \beta^2)^{1/2} \leq 1.82/\sqrt{2} = 1.29$ with superior dispersion characteristics relative to the SM2 scheme. On the other hand the LF4, TCT4Sm, and TCT4 schemes are stable for $c \leq 0.72/\sqrt{2}$, $c \leq 0.90/\sqrt{2}$ and $c \leq 1/\sqrt{2}$, respectively. For small values of α and β, scheme LF4 has a stability region whose contours are determined by the sum $\alpha + \beta$ approximately constant. It is seen from Figs. 4c, 4d, (respectively, Fig. 4e), and 4f that, as with second-order methods, stable regions are limited primarily by 4Δ (respectively, 8Δ) waves rather than by the shortest waves as is true for forward-in-time schemes.

In spite of the improved stability conditions of the advection characteristic methods, Figs. 5a–f show that these schemes do not significantly improve upon the dispersive phase errors. The dispersion characteristics associated with the TCT2 scheme reflect the second-order spatial differencing that it shares with the LF2 scheme. LF4 and TCT4 exhibit phase errors that are comparable in all essential respects with some slight differences. The TCT schemes are characterized by a mild deterioration in phase properties with increasing Courant number and the LF4 scheme is subject to very slight negative phase errors. The TCT4SM scheme is characterized by severe dispersion errors that plague both short- and medium-range waves, thereby removing this algorithm from serious consideration.

c. Rotational flow tests

The approximation schemes developed above were tested for the case of solid-body rotation. A standard cone distribution is advected about an axis through the origin with a pure rotational, nondivergent velocity field having an angular velocity of 0.25 rad s^{-1}. The computational domain consists of a uniform grid of 51×51 points ($\Delta x = 0.02$ and $\Delta y = 0.02$) and the initial distribution, which has unit height and a diameter of 0.16 is centered at $x_c = 0.5$ and $y_c = 0.34$ (see Fig. 6a). The nominal maximum Courant number, $(\alpha^2_{\max} + \beta^2_{\max})^{1/2}$, is equal to 0.60 and one full rotation around the origin requires 430 time steps. Time smoothing is implemented via an Asselin filter (Asselin 1972) with tunable coefficient ϵ as an option to remove the computational mode generated by the three time-level schemes being considered. Implementation of the TCT schemes at the boundaries follows standard higher-order methods, which consist of applying lower-order schemes at the boundary cells.

We shall consider, in addition to the time-centered schemes, several forward-in-time advection schemes that are commonly used in meteorological numerical models. In particular, the original Crowley scheme modified to include the cross-space term and reflect the dimensionality of the geometry (Smolarkiewicz 1982) and, for higher-order accuracy, Schlesinger's (1985) scheme 4 with type I correction (an upstream-biased, third-order phase correction) will be tested. These schemes will be designated CSM and SCH1, respectively.

Figure 6b presents the results after one full rotation for the LF2 scheme, which is equivalent to the conservative form of the classic second-order leapfrog scheme and should be compared to the scheme CSM (Fig. 6c). Both schemes are characterized by severe dispersive phase error that results from the space-centered approximation to the first partial derivatives. Despite neutral stability, dispersion of short waves leads to a maximum amplitude of 0.57 for the leapfrog scheme. The dissipative properties of the Crowley scheme, however, reduce the maximum amplitude to a value of 0.42. The Smolarkiewicz modification to leapfrog (SM2) (Fig. 6d) degrades the approximation by virtue of the severe short-wave dispersive error (as predicted by the linear analysis). The results at one rotation show an amplitude preservation of only 0.44 with extreme dispersion. One must, however, consider the expanded stability range afforded by this scheme. Dependence on Courant number is depicted in Table 3, which summarizes the cone test results for all schemes. The results for the TCT2, TCT4, and LF4 schemes are shown in Figs. 6e–g, and as can be seen, the TCT4 and LF4 schemes preserve both phase and amplitude well. TCT4 preserves 83% of the amplitude after one revolution and LF4 preserves 82%, with nearly identical dispersive patterns. These tendencies are clearly consistent with the linear stability

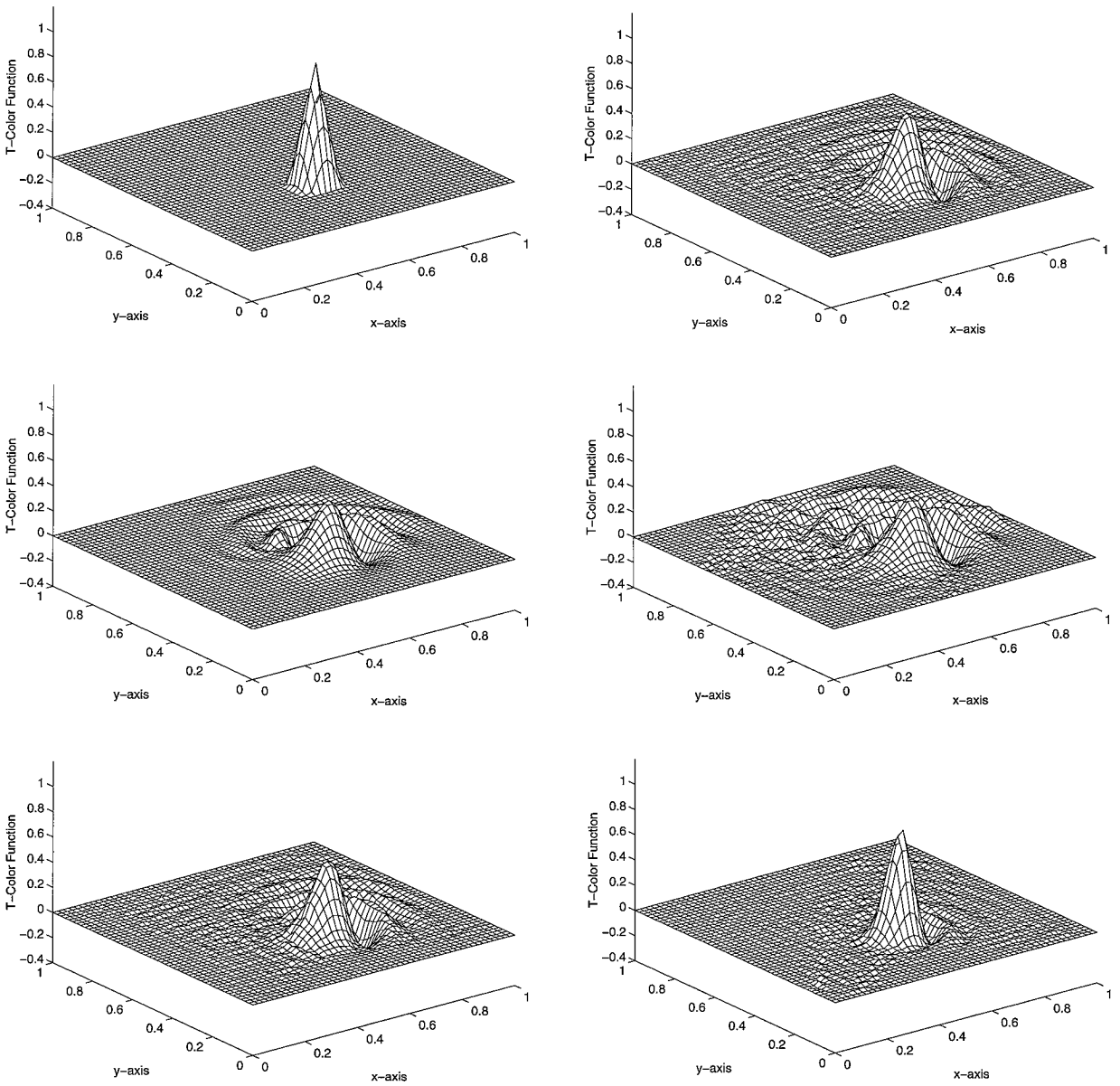

FIG. 6. Rotational flow tests (figures are labeled from upper left to lower right). Numerical solutions for CFL = 0.6 for various time-centered and forward-in-time schemes: (a) initial condition, (b) LF2, (c) CSM, (d) SM2, (e) TCT2, (f) TCT4, (g) LF4, and (h) Sch1. Numerical solutions at the stability limits for (i) LF2 at CFL = 0.8 and (j) TCT2 at CFL = 1.4. Numerical solutions for CFL = 0.6 for TCT conservative-flux schemes (k) FTCT2 and (l) FTCT4.

analysis. Very little dispersion is produced by Schlesinger's scheme that is based on a third-order phase correction. However, this scheme preserves only 53% of the amplitude after one revolution (see Fig. 6h).

The results for the fourth-order, centered-in-time schemes reflect the presence of short waves (2Δ–5Δ wavelength) propagating upstream because of the computational mode. Increasing the filter coefficient ϵ suppresses this mode with a maximum value of $\epsilon = 0.25$, effectively removing all stationary waves. Table 4 shows the influence of ϵ, which, in addition to smoothing dispersion error and to a lesser degree increasing dissipation, has a destabilizing effect. Referring again to Table 3, all schemes were tested, employing no filtering, for dependence on Courant number. A series of time steps yielding maximum Courant numbers of 0.6–1.6 were used. The SM2 scheme exhibits stable behavior for $c = 1.7$, surpassing all other schemes. However, as emphasized in the linear analysis and Fig. 6c, although the domain as a whole remains stable, dispersive waves severely degrade its performance. The superior stability characteristics of the TCT2 scheme are apparent as all other schemes (except SM2) exhibit highly unstable behavior at or below $c = 1.5$—a Courant number at which

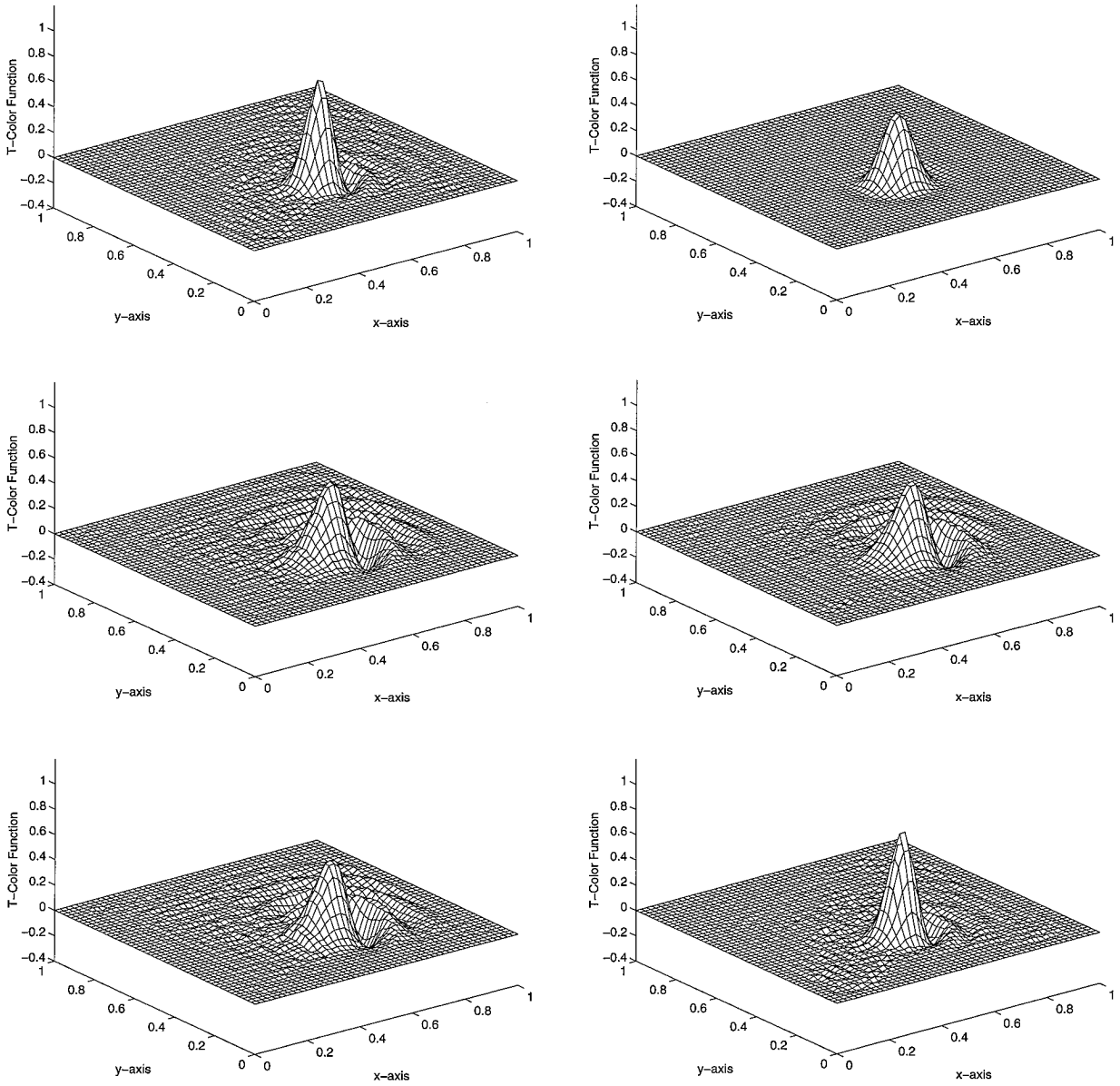

FIG. 6. (*Continued*)

it continues to perform stably. This particular scheme stands out as providing significantly enhanced stability characteristics with comparable accuracy to the popular LF2 scheme. Figures 6i and 6j compare the results of the LF2 and TCT2 schemes at their respective stability limits, that is, CFL = 0.8 and CFL = 1.4.

In section 3a conservative versions of the TCT schemes (denoted FTCT) are derived and the corresponding second-order algorithm is listed. These conservative algorithms have been applied to the solid-body rotation test and yield comparable results to the nonflux form (see Figs. 6k and 6l and Table 4). These results support the contention that the term of crucial importance on the right-hand side of Eq. (25) is

$$\mathbf{v}\mathbf{v}\cdot(\mathbf{v}\cdot\nabla)\nabla T,$$

and hence the FTCT difference approximations appropriately incorporate this effect. Moreover, we may identify this term with Dukowicz and Ramshaw's (1979) tensor viscosity term or Crowley's diffusion term, which have been shown to have an analogous stabilizing influence upon the canonical forward-in-time difference scheme.

4. Nonlinear advection

The effectiveness of the TCT schemes (relative to leapfrog methods) in solving the linear advection equa-

TABLE 3. Maximum and minimum of advected scalar T after one revolution of rotating cone as function of CFL number with Asselin filter off.

		CFL										
Scheme		0.6	0.7	0.8	0.9	1.0	1.1	1.2	1.3	1.4	1.5	1.6
LF2	max	0.5639	0.5656	0.5653	unstable	unstable	unstable	unstable	unstable	unstable	unstable	unstable
	min	−0.2194	−0.2275	−0.2258								
SM2	max	0.4373	0.4356	0.4348	0.4349	0.4357	0.4359	0.4350	0.4407	0.4402	0.4425	0.4430
	min	−0.2309	−0.2297	−0.2285	−0.2284	−0.2290	−0.2284	−0.2284	−0.2251	−0.2250	−0.2237	−0.2264
TCT4	max	0.8253	0.8211	0.8094	0.8024	0.7908	0.7872	unstable	unstable	unstable	unstable	unstable
	min	−0.1095	−0.1110	−0.1088	−0.1047	−0.1046	−0.1055					
TCT2	max	0.5638	0.5735	0.5740	0.5744	0.5717	0.5704	0.5673	0.5622	0.5609	unstable	unstable
	min	−0.2107	−0.2095	−0.2126	−0.2162	−0.2228	−0.2221	−0.2187	−0.2168	−0.2234		
LF4	max	0.8196	unstable	unstable	unstable	unstable	unstable	unstable	unstable	unstable	unstable	unstable
	min	−0.0988										
CSM	max	0.4183	0.4152	0.4111	0.4083	0.4009	0.3991	unstable	unstable	unstable	unstable	unstable
	min	−0.2059	−0.2030	−0.2001	−0.1966	−0.1991	−0.1900					
Sch1	max	0.5313	0.5324	0.5326	0.5335	unstable	unstable	unstable	unstable	unstable	unstable	unstable
	min	−0.0231	−0.0227	−0.0222	−0.0407							

tion does not certify them for general use. In realistic atmospheric problems the momentum equations exhibit highly nonlinear behavior and methods preferable for scalar equations may perform poorly. In particular, the approximation of highly nonlinear convection terms like $u\partial u/\partial x$ is problematic, especially for nonconservative schemes (in the context of highly nonlinear atmospheric models, the treatment of certain equations requires the conservation of quadratic quantities). In the next section we shall confirm the linear results for the case of Burger's equation in one dimension. This equation is a prototype equation for the nonlinear momentum equations. It will be shown, however, that when applied in its conservative form the TCT2 scheme appears to be superior to the second-order leapfrog scheme in its treatment of nonlinear equations.

In this section we will compare the results obtained by the conservative leapfrog scheme and the proposed TCT method when nonlinear systems are solved. Initially, we will consider the following 1D nonlinear wave equation:

$$\frac{\partial u}{\partial t} + u\frac{\partial u}{\partial x} = \frac{\partial u}{\partial t} + \frac{\partial F}{\partial x} = 0, \tag{30}$$

where $F = u^2/2$. This equation is referred to as the inviscid Burger's equation and describes a wave in which each point may have different phase speed. Equation (30) describes how an initial distribution steepens in regions of negative gradients and levels off in regions of positive gradients. For an initial distribution characterized by a steep negative gradient (see Fig. 7a) the analytical solution develops a mathematical discontinuity similar to a shock wave in supersonic flows. In this case numerical solutions will not converge unless sufficient implicit numerical viscosity is introduced, as usually encountered in the approximation of localized phenomena of atmospheric problems.

TABLE 4. Maximum and minimum of advected scalar T after one revolution of rotating cone as function of the Asselin filter parameter with Courant number $\alpha = 0.6$.

		ϵ			
Scheme		0	0.1	0.2	0.25
LF2	max	0.5639	0.5426	0.5182	0.5046
	min	−0.2194	−0.1954	−0.1749	−0.1641
SM2	max	0.4373	0.4264	0.4143	0.4092
	min	−0.2309	−0.2210	−0.2129	−0.2093
TCT4	max	0.8253	0.7502	0.6894	0.6600
	min	−0.1095	−0.0629	−0.0445	−0.0417
TCT2	max	0.5638	0.5442	0.5203	0.5069
	min	−0.2107	−0.1926	−0.1739	−0.1636
LF4	max	0.8196	0.7646	unstable	unstable
	min	−0.0988	−0.1584		

The second-order leapfrog scheme applied to the 1D nonlinear wave equation can be expressed as

$$\mathrm{flx}_j^n = \left[0.5\left(\frac{u_j^n + u_{j-1}^n}{2}\right)^2\right],$$

$$u_j^{n+1} - u_j^{n-1} = -\frac{2\Delta t}{\Delta x}(\mathrm{flx}_{j+1}^n - \mathrm{flx}_j^n). \tag{31}$$

The nonlinear version of the TCT2 scheme is based on the conservative flux form. Discretizing in time yields

$$\frac{u^{n+1} - u^{n-1}}{2\Delta t} = -\frac{\partial F}{\partial x}, \tag{32}$$

where $F = u^2/2$. As with the linear case, we introduce forward-time and backward-time Taylor expansions,

$$(u_t)^n = \frac{u^{n+1} - u^{n-1}}{2\Delta t} - \frac{\Delta t^3}{6}(u_{ttt})^n,$$

TABLE 5. Maximum and minimum of advected scalar T for the flux-conservative TCT schemes after one revolution of rotating cone as function of CFL number with Asselin filter off.

		CFL										
Scheme		0.6	0.7	0.8	0.9	1.0	1.1	1.2	1.3	1.4	1.5	1.6
FTCT2	max	0.5587	0.5641	0.5716	0.5729	0.5653	0.5709	0.5677	0.5579	0.5563	0.5593	unstable
	min	−0.2133	−0.2118	−0.2124	−0.2144	−0.2151	−0.2177	−0.2166	−0.2099	−0.2115	−0.2139	
FTCT4	max	0.8104	0.8163	0.8146	0.8138	0.7898	0.7833	unstable	unstable	unstable	unstable	unstable
	min	−0.1029	−0.1060	−0.1090	−0.1089	−0.1033	−0.1026					

and a semidiscrete approximation to Eq. (30) at time level n is

$$\frac{u^{n+1} - u^{n-1}}{2\Delta t} = -\frac{\partial F}{\partial x} + \frac{\Delta t^2}{6} u_{ttt}. \tag{33}$$

Successive approximations using Eq. (30) yields

$$\frac{\partial^2 u}{\partial t^2} = \frac{\partial}{\partial x}\left(u\frac{\partial F}{\partial x}\right) \quad \text{and} \quad \frac{\partial^3 u}{\partial t^3} = -\frac{\partial^3 (F^2)}{\partial x^3}. \tag{34}$$

Combining Eqs. (33) and (34) the semidiscrete approximation may be replaced by

$$\frac{u^{n+1} - u^{n-1}}{2\Delta t} = \frac{\partial F^n}{\partial x} - \frac{\Delta t^2}{6}\frac{\partial^3 (F^2)^n}{\partial x^3},$$

or in conservative flux form

$$\frac{u^{n+1} - u^{n-1}}{2\Delta t} = \left(\frac{\partial \mathcal{F}}{\partial x}\right)^n,$$

where

$$\mathcal{F} = F - \frac{\Delta t^2}{6}\frac{\partial^2 (F^2)}{\partial x^2}.$$

Finally, to obtain a fully discrete equation we apply centered differences to the spatial derivatives, employing second-order accurate approximations. This scheme can be expressed as

$$\mathrm{fl}x_j^n = \left\{0.5u_j^{n2} - \frac{\Delta t^2}{6} \times \frac{[(0.5u_{j+1}^n{}^2)^2 - 2(0.5u_j^{n2})^2 + (0.5u_{j-1}^n{}^2)^2]}{\Delta x^2}\right\}.$$

We shall compare the performance of the second-order time-centered schemes described above with the MacCormack scheme (MacCormack 1969), a two-step, Lax–Wendroff-type finite difference technique widely used in aerospace simulations. Mendez-Nunez and Carroll (1993) compared the MacCormack scheme with second-order leapfrog and positive-definite Smolarkiewicz

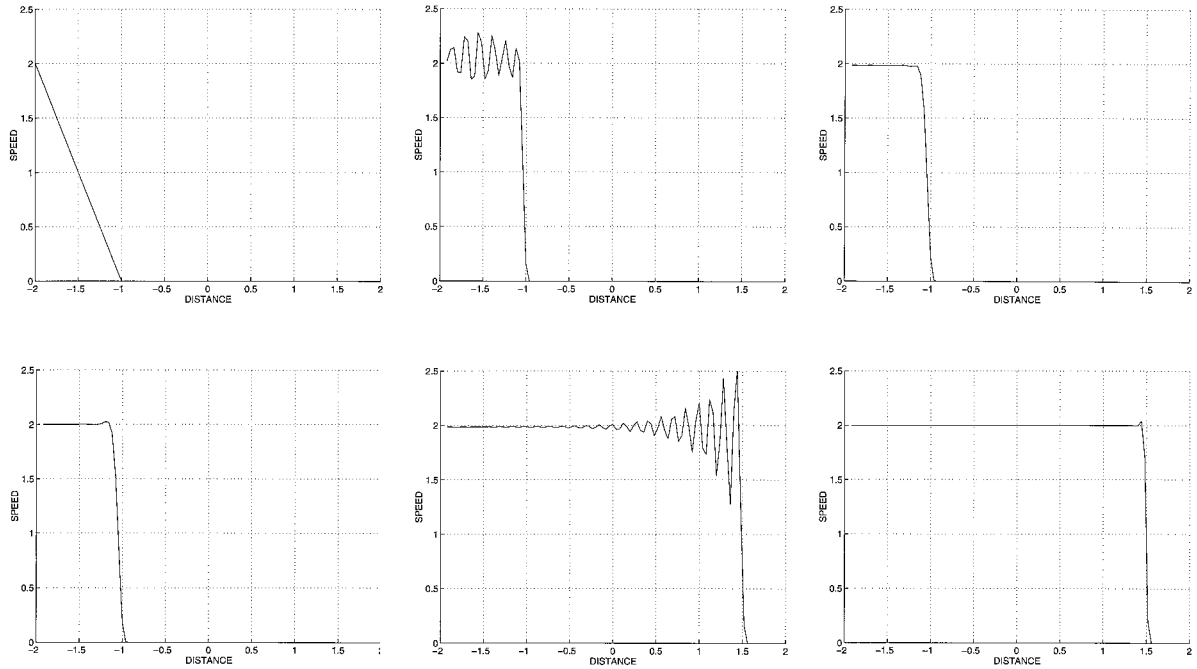

FIG. 7. Numerical solutions of the 1D inviscid Burger's equation by leapfrog, TCT, and MacCormack schemes for moderately steep negative gradient at CFL = 0.8 shown at 30 and 187 time steps (labels from upper left to lower right): (a) initial condition, (b) LF2 at 30 time steps, (c) FTCT2 at 30 time steps, (d) MacCormack at 30 time steps, (e) FTCT2 at 187 time steps, and (f) MacCormack at 187 time steps.

(1985) for solving the nonlinear advection equation and found it to be superior based on a variety of stability criteria. Chief among these was the modest amounts of numerical diffusion (an advantage when treating problems involving steep gradients) that permitted damping of high-frequency oscillations that characteristically arise in approximating nonlinear phenomena. In addition, the MacCormack scheme behaves well for larger CFL numbers, while LF2 produced better results for smaller CFL numbers. Although a portion of our results, in effect, reproduce the work of Mendez-Nunez and Carroll, it is the comparison of the TCT scheme that we are emphasizing both relative to leapfrog and the MacCormack schemes.

We first compare the behavior of the various schemes using an initial disturbance spread across 25 grid points located between grid points 0 and 25 in a 100-point domain (see Fig. 7a). Time smoothing is implemented for the time-centered schemes via the Asselin filter with coefficient $\epsilon = 0.25$. The analytical solution moves at a speed proportional to height across the wave front; hence, the initial gradient steepens with time. Boundary values are constrained to the analytical solution and integration times are limited to avoid boundary effects. Emphasizing large CFL number behavior, numerical results for an initial CFL = 0.8 are shown in Figs. 7b–f. Each scheme exhibits some numerical dispersion with the MacCormack scheme producing modest amounts of implicit numerical diffusion. Diffusion may be identified with a spreading of the steep gradient zone at the downstream side and also intrinsic damping of the computationally generated modes. Numerical dispersion is reflected in the overshoot immediately upstream of the steep gradient with accompanying oscillations. For time-centered schemes (i.e., both leapfrog and TCT) we would expect the presence of high-frequency oscillations mollified by the application of Asselin smoothing filters. These essentially nonlinear phenomena become increasingly important relative to the linear dispersion effects predicted in the stability analysis of section 3b. The number and magnitude of the high-frequency oscillations in the leapfrog solution are significantly greater than the MacCormack scheme (as shown by Mendez-Nunez and Carroll) as well as the TCT schemes (compare Figs. 7b–d). Mendez-Nunez and Carroll attribute the MacCormack result to its intrinsic diffusion. However, the TCT result must be associated with the stabilizing effect of the higher-order temporal term that was evident in the linear results. Comparison of the results generated by the MacCormack scheme (which is recommended by Mendez-Nunez and Carroll for nonlinear equations) and those of the TCT2 scheme are striking—both exhibit a very modest overshoot with negligible upstream oscillations.

If integration is carried out far enough in time the gradient steepens to a virtual discontinuity. The MacCormack and FTCT2 schemes remain stable over such long-term integration times (see Figs. 7e and 7f) that, since we are neglecting diffusion, the near-shock conditions lead to numerical dispersion, which particularly distorts the TCT2 solution.

TABLE 6. Nonlinear stability as a function of initial maximum Courant number for compression wave.

Scheme	Initial CFL			
	0–0.7	0.8–1.0	1.1–1.3	1.4–∞
LF2	stable	unstable	unstable	unstable
TCT2	stable	stable	stable	unstable
MacCormack	stable	stable	unstable	unstable

The influence of the CFL number on the stability (boundedness) of the solutions was examined by considering the same initial disturbance and varying the time step while integrating over 1.75 time units. Qualitative results that indicate the boundedness of the solution over the course of long-term integration are shown in Table 6. Stability limits for the leapfrog and MacCormack's scheme are consistent with previous results, while the TCT2 scheme exhibits bounded solutions for significantly larger CFL numbers (stability is defined for CFL $\leq$ 1.4).

The inverse phenomenon to a continually steepening waveform (i.e., shock), more common in atmospheric flows, is that of a positive gradient weakening with time (i.e., rarefaction). The approximate solution to Eq. (30), obtained with each of the schemes (with an initial disturbance as in Fig. 8a), exhibits the same qualitative behavior as for the steepening gradient case with the leapfrog algorithm plagued by high-frequency oscillations. Figures 8b–d show the solution obtained at one time unit with the leapfrog, TCT2, and MacCormack schemes, respectively. Mendez-Nunez and Carroll (1993) found that for Courant numbers greater than 0.5 the leapfrog scheme invariably induces large oscillations and suggest that, in real flow simulations in which weakening gradients are likely to occur, the CFL number should be reduced. The TCT2 and MacCormack schemes again perform quite well, yielding proper wave speed with some spreading of the discontinuity and a modest amount of numerical dispersion. Table 7 provides an indication of the boundedness of solutions over a range of CFL numbers (for an integration time of one unit). The enhanced stability characteristics associated with the TCT2 scheme are striking. In fact, when applied to the evolving rarefaction wave the maximum CFL number compatible with stability exceeds that associated with the LF2 scheme by a factor of 2 while exceeding that associated with MacCormack's scheme by 55%.

5. Summary

The goal of this paper was to describe and examine the effectiveness of time-centered advection algorithms employed in explicit atmospheric models. The standard

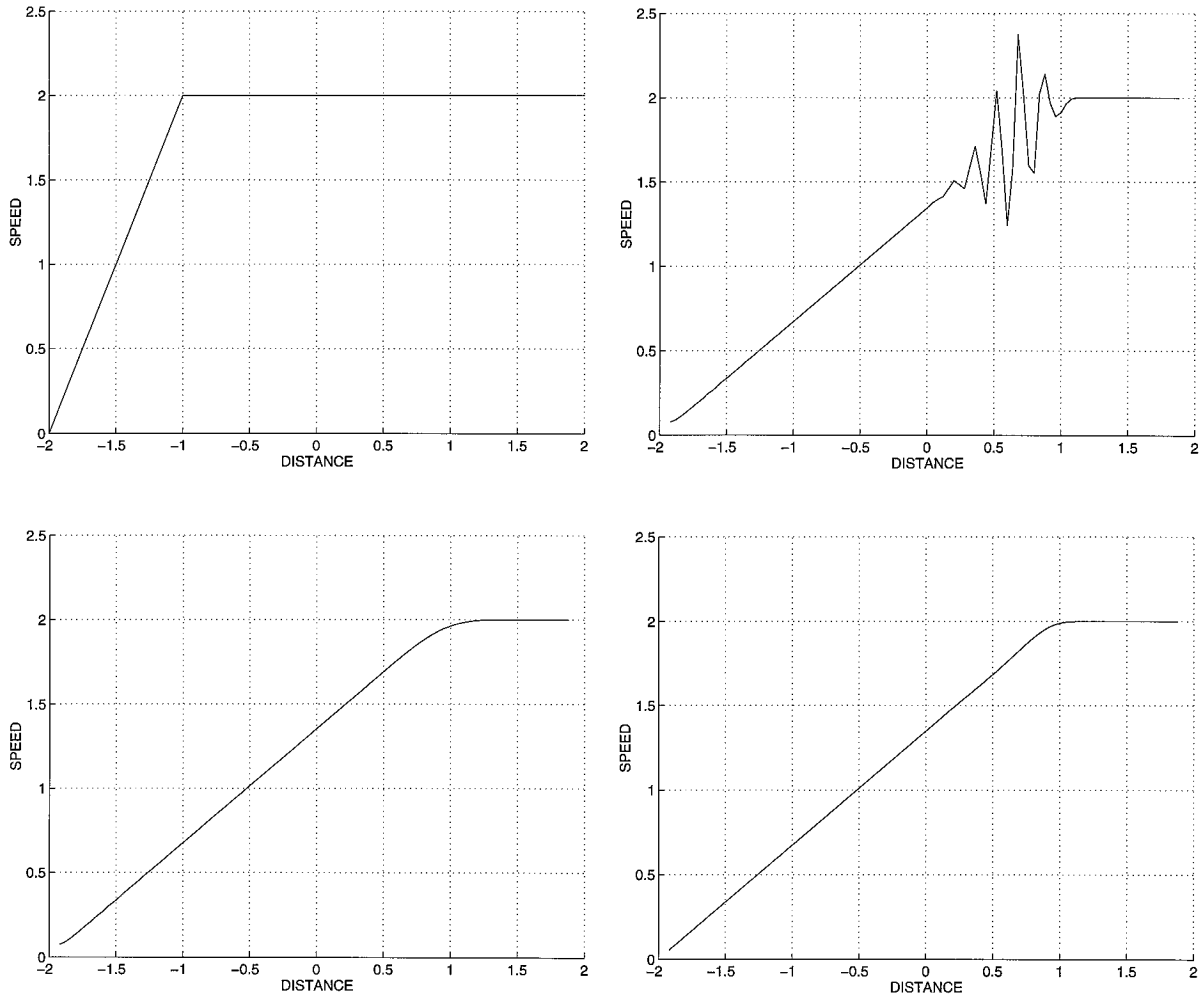

FIG. 8. Numerical solutions of the 1D inviscid Burger's equation by leapfrog, TCT, and MacCormack schemes for moderately steep positive gradient at CFL = 0.9 shown at 30 time steps (labels from upper left to lower right): (a) initial condition, (b) LF2 at 30 time steps, (c) FTCT2 at 30 time steps, and (d) MacCormack at 30 time steps.

techniques consist of second-order and fourth-order forms of the conservative leapfrog scheme. At the same time we considered alternative algorithms consistent with this formulation, that is, explicit and time-centered, and present a detailed comparison with the leapfrog schemes.

Applying standard second-order time-differencing to hyperbolic equations (i.e., which characterize convection-dominated atmospheric flows) invariably results in rather severe stability restrictions. The primary problem appears to be attributable to the differencing approximation of the time derivative term (Donea 1984). We have shown in this paper that producing higher order temporal accuracy (TCT) results in schemes with improved stability properties compared with conventional leapfrog methods.

TABLE 7. Nonlinear stability as a function of initial maximum Courant number for rarefaction wave.

Scheme	Initial CFL			
	0–0.8	0.9–1.1	1.2–1.7	1.8–∞
LF2	stable	unstable	unstable	unstable
TCT2	stable	stable	stable	unstable
MacCormack	stable	stable	unstable	unstable

The linear results show that marked improvement is possible in the stability properties of explicit, time-centered advection schemes by including, in the differencing scheme, a crucial term approximating the time derivative of third order. The critical CFL number for the TCT2 scheme was shown to exceed that of LF2 by nearly a factor of 2. Similar results hold for the corresponding fourth-order schemes. A simpler but significantly more dispersive scheme is obtained by Shuman averaging (Smolarkiewicz 1982). This scheme was characterized by the largest maximum critical CFL number surpassing even the TCT2. The solid body rotation test (section 3c) confirmed the findings of the 2D sta-

bility analysis and compared these time-centered schemes with popular forward-in-time methods.

The 1D nonlinear results corroborate the fundamental stabilizing effect of the TCT approach with the stability range of the conservative TCT2 algorithm exceeding leapfrog by a factor of 2 and MacCormack's scheme, a popular nonlinear, dissipative differencing scheme (see Mendez-Nunez and Carroll), by 50%.

On the basis of the results presented in this paper the TCT methods represent an attractive alternative to the leapfrog schemes currently used in many explicit, time-centered models where stability considerations are critical.

Acknowledgments. The authors would like to extend a special thanks to Richard Ewing and Lance O'Steen for discussions concerning advection processes in mesoscale computations. In addition, the authors are grateful to Jim Sochacki, Patrick O'Leary, Al Bessey, and Bob Ribando for the computational assistance they provided during the early stages of this work. Finally, the authors acknowledge that many constructive remarks of the referees' were used to improve an earlier version of this paper.

REFERENCES

Asselin, R. A., 1972: Frequency filter for time integrations. *Mon. Wea. Rev.,* **100,** 487–490.

Bird, R. B., W. E. Stewart, and E. N. Lightfoot, 1960: *Transport Phenomena.* John Wiley, 780 pp.

Crowley, W. P., 1968: Numerical advection experiments. *Mon. Wea. Rev.,* **96,** 1–11.

Donea, J., 1984: A Taylor–Galerkin method for convective transport problems. *Int. J. Numer. Methods Fluids,* **20,** 101–119.

Douglas, J., Jr., and T. F. Russell, 1982: Numerical methods for convection-dominated diffusion problems based on combining the method of characteristics with finite element or finite difference procedures. *SIAM J. Numer. Anal.,* **19,** 871–875.

Dukowicz, J. K., and J. D. Ramshaw, 1979: Tensor viscosity method for convection in numerical fluid dynamics. *J. Comput. Phys.,* **32,** 71–79.

Fromm, C. K., 1968: A method for reducing dispersion in convective difference schemes. *J. Comput. Phys.,* **3,** 176–189.

Haltiner, G. J., and R. T. Williams, 1980: *Numerical Prediction and Dynamic Meteorology.* John Wiley, 477 pp.

Leith, C. E., 1965: Numerical simulation of the earth's atmosphere. *Methods Comp. Phys.,* **4,** 1–28.

MacCormack, R. W., 1969: The effect of viscosity in hypervelocity impact cratering. AIAA Paper 69-354.

Mendez-Nunez, L. R., and J. J. Carroll, 1993: Comparison of leapfrog, Smolarkiewicz, and MacCormack schemes applied to nonlinear equations. *Mon. Wea. Rev.,* **121,** 565–578.

Raithby, G. D., 1976: A critical evaluation of upstream differencing applied to problems involving fluid flow. *Comput. Methods Appl. Mech. and Eng.,* **9,** 75–103.

Schlesinger, R. E., 1985: Effects of upstream-biased third-order space correction terms on multidimensional Crowley advection schemes. *Mon. Wea. Rev.,* **113,** 1109–1130.

Smolarkiewicz, P. K., 1982: The multidimensional Crowley advection scheme. *Mon. Wea. Rev.,* **110,** 1968–1983.

——, 1985: On the accuracy of the Crowley advection scheme. *Mon. Wea. Rev.,* **113,** 1425–1429.

Strikwerda, J. C., 1989: *Finite Difference Schemes and Partial Differential Equations.* Wadsworth & Brooks/Cole, 386 pp.